

Fluorescence Characterization of the Hydrophobic Pocket of Cyclophilin B

J. R. Albani · M. Carpentier · C. Lansiaux

Received: 2 June 2007 / Accepted: 10 August 2007 / Published online: 25 September 2007
© Springer Science + Business Media, LLC 2007

Abstract Human cyclophilin B is a monomeric protein that contains two tryptophan residues, Trp104 and 128. Trp128-residue belongs to the binding site of cyclosporin A and is the homologous of Trp 121 in CyPA, while Trp104 residue belongs to the hydrophobic pocket. In the present work, we studied the dynamics of Trp residue(s) of cyclophilin B and of the CyPB_{w128A} mutant and of TNS-mutant complex. Our results showed that Trp-104 and TNS show restricted motions within their environments and that energy transfer between the two fluorophores is occurring.

Keywords Cyclophilin B · Trp residues · 2-*p*-toluidinylnaphthalene-6-sulfonate (TNS) · Red-edge excitation spectra · Fluorescence anisotropy · Fluorescence lifetimes · Quantum yield · Emission to excitation ratio

Abbreviations

a.u. arbitrarily scaled units
CsA cyclosporin A
hCyPB human cyclophilin B

Introduction

Cyclophilins are highly conserved proteins that are present in many types of cells with a considerably divergent phylogenetic distribution [1]. Several cyclophilin isoforms with distinct subcellular localizations have been described, cyclophilin A, B and C. Cyclophilin A (CyPA) (18 kDa) is an abundant cytosolic protein [2]. The 22-kDa cyclophilin B (CyPB) is located in the endoplasmic reticulum and shares 64% sequence identity to CyPA [3]. Cyclophilin C (CyPC) (23 kDa) shares 55.8% sequence identity to CyPA and was found to be particularly abundant in kidneys [4]. Also, cyclophilins B and C contain an N-terminal signal sequence thought to mediate translocation into the endoplasmic reticulum [3–6]. Finally, there is cyclophilin D (CyPD) that is a mitochondrial protein [7, 8]. Cyclophilins A, B and C could be involved in degradation of the genome during apoptosis [9], and cyclophilin D plays a role in the mitochondrial permeability transition [10].

Human cyclophilins belong to the family of peptidyl-prolyl *cis*–*trans* isomerases (PPIases). PPIases catalyse the interconversion of the *cis* and *trans* isomers of the peptidyl-prolyl bonds in peptide and protein substrates [11, 12]. The potent and clinically useful immunosuppressant cyclosporin A (CsA) binds to human Cyclophilins, inducing in this way an important inhibition of their enzymatic activity [2, 13]. Recent work has shown that the binding site of CsA on cyclophilin B and the catalytic site of the protein are distinct [14].

Human cyclophilin B is a monomeric protein consisting of 183 amino acids and containing two tryptophan residues, Trp104 and 128. Trp128-residue belongs to the binding site of cyclosporin A and is the homologous of Trp 121 in CyPA, while Trp-104 residue belongs to the hydrophobic pocket. The two sites are localized in a large hydrophobic

J. R. Albani (✉) · C. Lansiaux
Laboratoire de Biophysique Moléculaire,
Université des Sciences et Technologies de Lille, Bât. C6,
59655 Villeneuve d'Ascq Cédex, France
e-mail: Jihad-Rene.Albani@univ-lille1.fr

M. Carpentier
Unité de Glycobiologie structurale et fonctionnelle,
UMR n° 8576, Université des Sciences et Technologies de Lille,
59655 Villeneuve d'Ascq Cédex, France

pocket [15]. The CyPB_{w128A} mutant is unable to interact with CsA, demonstrating that the requirement of this amino acid residue in the interactions with the drug is also a common feature of CyPA and CyPB. However, the CyPB_{w128A} mutant retains 60% of the capacity to accelerate the *cis*–*trans* isomerization of a Pro-containing substrate, indicating that the Trp-128 residue in CyPB was not essential for PPIase activity. This is not the case for CyPA where mutation of the corresponding Trp-121 residue was reported to strongly reduce the enzymatic activity [14].

Fluorescence spectroscopy allows obtaining information on the structure and dynamics of proteins. Intrinsic fluorophore such as Trp residues [16, 17] or extrinsic ones such as 2-*p*-toluidinylnaphthalene-6-sulfonate (TNS) [18, 19] can be used.

The dynamics of proteins are currently investigated by fluorescence anisotropy studies and by the red-edge excitation spectra method [20, 21]. Excitation at the red-edge of the absorption spectrum of the fluorophore molecules allows one to study the flexibility of their microenvironment. In the presence of local motion, the position of the maximum of the fluorescence spectrum of the fluorophore does not vary with the excitation wavelength. However, in a viscous or rigid medium, the fluorescence maximum position shifts to higher wavelengths upon red-edge excitation. Anisotropy studies allow one to monitor the dynamics of the fluorophore itself [22]. Thus both techniques are complementary, but different types of information are collected.

In the present work, we studied the dynamics of Trp residue(s) of cyclophilin B and of the CyPB_{w128A} mutant and of TNS–mutant complex. Also, binding parameters (stoichiometry and dissociation constant) of the TNS–CyPB_{w128A} mutant complex are reported. Our results show that fluorescence of Trp-128 residue is weak and Trp-104 and TNS show restricted motions within their environments. Quenching of fluorescence intensity of Trp 104 of CyPB_{w128A} mutant by TNS indicates that energy transfer occurs between the two fluorophores.

Materials and methods

Recombinant human CyPB was purified as previously described [6].

The CyPB_{w128A} mutant was generated using the Quick-change kit (Stratagene, La Jolla, CA) with minor modifications. Briefly, complementary primers covering the region to be substituted was used to generate mutated, unmethylated strands. Upon treatment with the *DpnI* endonuclease twice for three hours at 37°C, the methylated template DNA was digested allowing the selective rescue of the mutated strand after bacterial transformation. The DNA sequence of the mutant plasmid was verified using the

dideoxy chain termination method [23]. Purification of CyPB_{w128A} mutant protein was performed as for wild type CyPB using the procedure described in [6]. Based on the amino acid composition [24], calculated extinction coefficients at 280 nm are 15.980 M⁻¹ cm⁻¹ for the wild-type and 10.420 M⁻¹ cm⁻¹ for the mutant.

The concentration of TNS (from Sigma) was determined spectrophotometrically using an extinction coefficient equal to 18.9 mM⁻¹ cm⁻¹ at 317 nm [25].

The stock solution of CsCl (from Sigma) was 4 M.

Absorbance data were obtained with a Shimadzu MPS-2000 spectrophotometer using 1-cm pathlength cuvettes.

Fluorescence spectra were recorded with a Perkin-Elmer LS-5B spectrofluorometer. The bandwidths used for the excitation and the emission were 5 nm. The quartz cuvettes had optical pathlengths equal to 1 and 0.4 cm for the emission and excitation wavelengths, respectively. Observed fluorescence intensities were corrected for absorption as described in [26, 27]. Finally, fluorescence spectra were corrected for the background intensities of the buffer solution.

The Perrin plot was obtained from anisotropy data measured with the same instrument, ($\lambda_{\text{ex}}=300$ and $\lambda_{\text{em}}=330$ nm). The bandwidths used for the excitation and the emission were 10 nm. Values of the anisotropy (*a*) were obtained from parallel and perpendicular fluorescence intensities after subtraction of the Raman signal of the buffer solution. The bandwidths used for both the excitation and the emission were 10 nm.

Fluorescence lifetime measurements were obtained with a Horiba Jobin Yvon FluoroMax-4P, using the time correlated single photon counting method. Excitation was performed at 295 nm with a nanoLED and emission was observed at 330 nm for the Trp residues in both proteins and at 420 nm for TNS.

Quantum yields of the wild-type and of the mutant were determined relative to tryptophan in water according to [28]

$$Q_{\text{prot}} = \frac{A_{\text{Trp}} \sum I_{\text{prot}}}{A_{\text{prot}} \sum I_{\text{Trp}}} Q_{\text{Trp}} \quad (1)$$

where $\sum I$ is the integrated intensity over the wavelength region 300–400 nm, *A* is the absorbance at 295 nm, and the quantum yield Q_{Trp} for tryptophan in water is taken as 0.14 [28].

Results

Fluorescence emission spectra and quantum yields of Trp residues in wild type cyclophilin B and mutant CyPB_{w128A}

Figure 1 displays the normalized fluorescence emission spectra of wtCyPB (a) and mutant CyPB_{w128A} (b). The wild type shows an emission spectrum with a maximum located

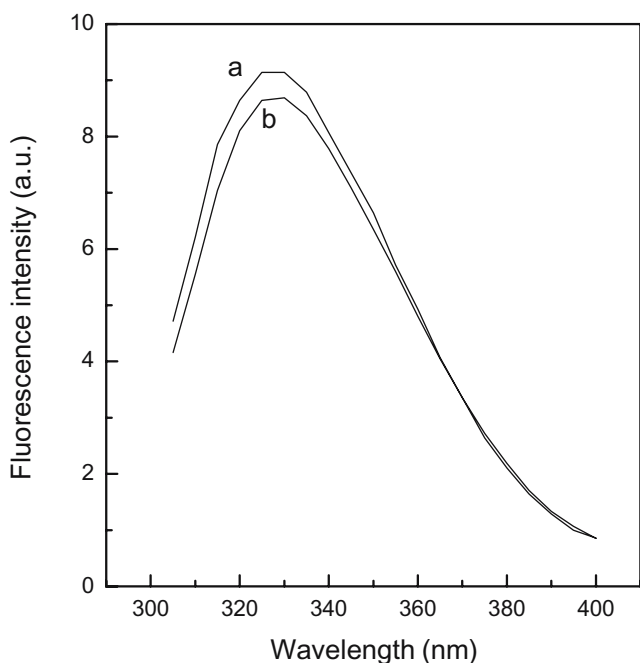


Fig. 1 Normalized fluorescence emission spectra of wtCyPB (a) and of mutant CyPB_{w128A} (b), both normalized for the same optical density (0.01) at the excitation wavelength (295 nm) and recorded in 10 mM PBS buffer, pH 7 at $\lambda_{ex}=295$ nm. The wild type shows an emission spectrum with a maximum located at 329 ± 1 nm and a bandwidth equal to 53 ± 1 nm. The mutant cyclophilin B possesses an emission spectrum with a peak at 326 ± 1 nm and a bandwidth of 45 ± 1 nm. The quantum yields of Trp residues of the wild type and of the mutant are equal to 0.061 and 0.049, respectively

at 329 ± 1 nm and a bandwidth equal to 53 ± 1 nm. The position of the maximum is characteristic of an emission from embedded Trp residues; however the value of the bandwidth indicates that two classes of Trp residues (embedded and surface) contribute to the emission of the wild type.

The mutant cyclophilin B possesses an emission spectrum with a peak at 327 ± 1 nm and a bandwidth of 45 ± 1 nm. This is characteristic of a fluorescence emission from Trp residue embedded in the protein matrix [29]. The quantum yields of Trp residues of the wild type and of the mutant are equal to 0.061 and 0.049, respectively. Therefore, Trp-128 residues in the wild type would display 19% of the total fluorescence of the wild type. This could be true if the quantum yields are considered as additive (see discussion).

Addition of a selective quencher such as CsCl at high concentration (2M) inhibits the fluorescence emission of the surface Trp residue and allows obtaining the fluorescence emission spectrum of the buried Trp residue [30]. Figure 2 shows the emission spectra of wtCyPB in absence (a) and in presence (b) of 2M CsCl. Spectrum b character-

izes the emission of the buried Trp residue ($\lambda_{max}=324$ nm) with a quantum yield equal to 0.054. The emission spectrum of the quenched Trp-residue (Trp-128 residue) (c) is obtained by subtracting spectrum (b) from (a). The emission maximum of the accessible Trp-residue is located at 350 nm, a characteristic of an emission from a Trp residue at the surface of the protein. As a test experiment, we recorded the fluorescence emission spectrum of the mutant CyPB_{w128A} in the absence and in the presence of CsCl. After corrections for the dilution, we did not observe any variation in the fluorescence data (Fig. 3).

Lifetime data

Fluorescence intensity, $I(\lambda, t)$, of Trp residues in wild type cyclophilin B can be adequately represented by a sum of three exponentials

$$I(\lambda, t) = 0.214 e^{-t/0.684} + 0.603 e^{-t/1.784} + 0.183 e^{-t/4.376}$$

where 0.214, 0.603 and 0.183 are the pre-exponential factors, 0.684 ± 0.09 , 1.784 ± 0.07 and 4.736 ± 0.12 ns are the decay times and λ is the emission wavelength (330 nm) ($\chi^2=$

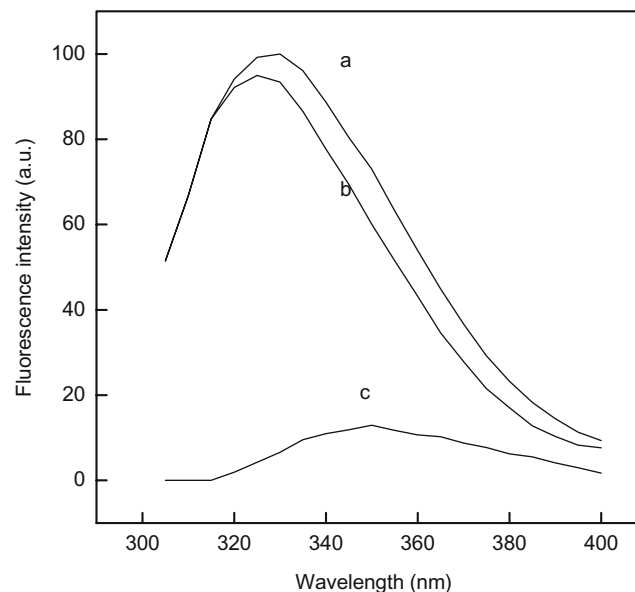


Fig. 2 Fluorescence emission spectra of wtCyPB in absence (a) and in presence (b) of 2 M cesium, obtained in 10 mM PBS buffer, pH 7 at $\lambda_{ex}=295$ nm. Spectrum b characterizes the emission of the buried Trp residue ($\lambda_{max}=324$ nm) with a quantum yield equal to 0.054. The emission spectrum of the quenched Trp-residue (Trp-128 residue) (c) is obtained by subtracting spectrum (b) from (a). The emission maximum of the accessible Trp-residue is located at 350 nm, a characteristic of an emission from a Trp residue at the surface of the protein

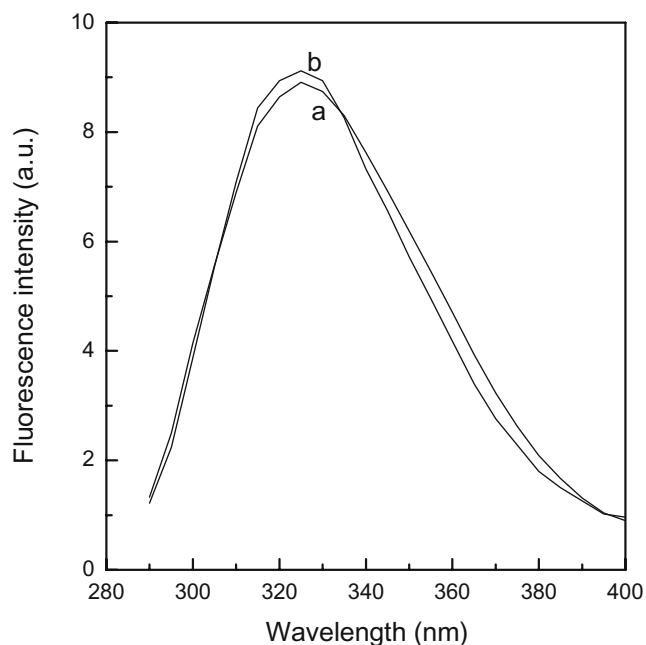
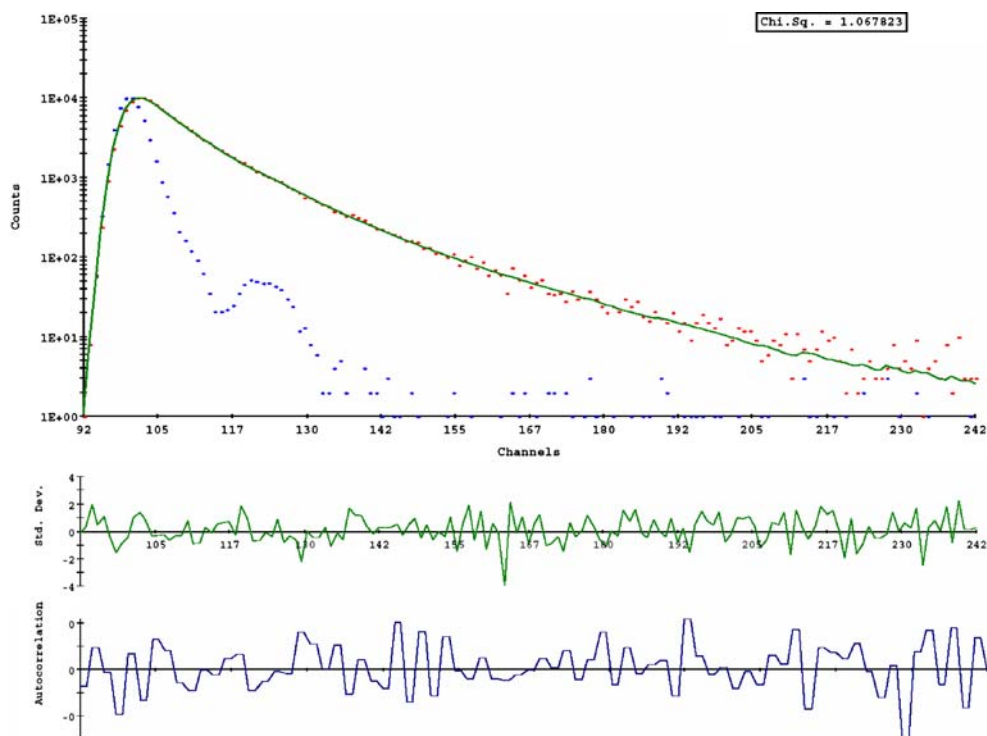


Fig. 3 Fluorescence emission spectra of mutant cyclophilin B in the absence (a) and in the presence (b) of 2 M cesium. $\lambda_{\text{ex}}=280$ nm. There is no shift in the emission peak and no intensity decrease as it is observed for the wild type. The intensity is slightly higher in presence of cesium probably due to the error in the dilution

Fig. 4 Fluorescence intensity decay of wild type cyclophilin B. $\lambda_{\text{ex}}=295$ nm and $\lambda_{\text{em}}=330$ nm



1.067). $\lambda_{\text{ex}}=295$ nm (Fig. 4). The weighted average fluorescence lifetime $\langle\tau\rangle=2.9$ ns was used to calculate the rotational correlation time from the Perrin plot.

$$\langle\tau\rangle = \sum f_i \tau_i \quad (2)$$

and

$$f_i = \alpha_i \tau_i / \sum \alpha_i \tau_i \quad (3)$$

where α_i are the pre-exponential terms and τ_i are the fluorescence lifetimes.

The fluorescence intensity decay of Trp-104 residue in the mutant CyPB_{W128A} can also be adequately represented by a sum of three exponentials

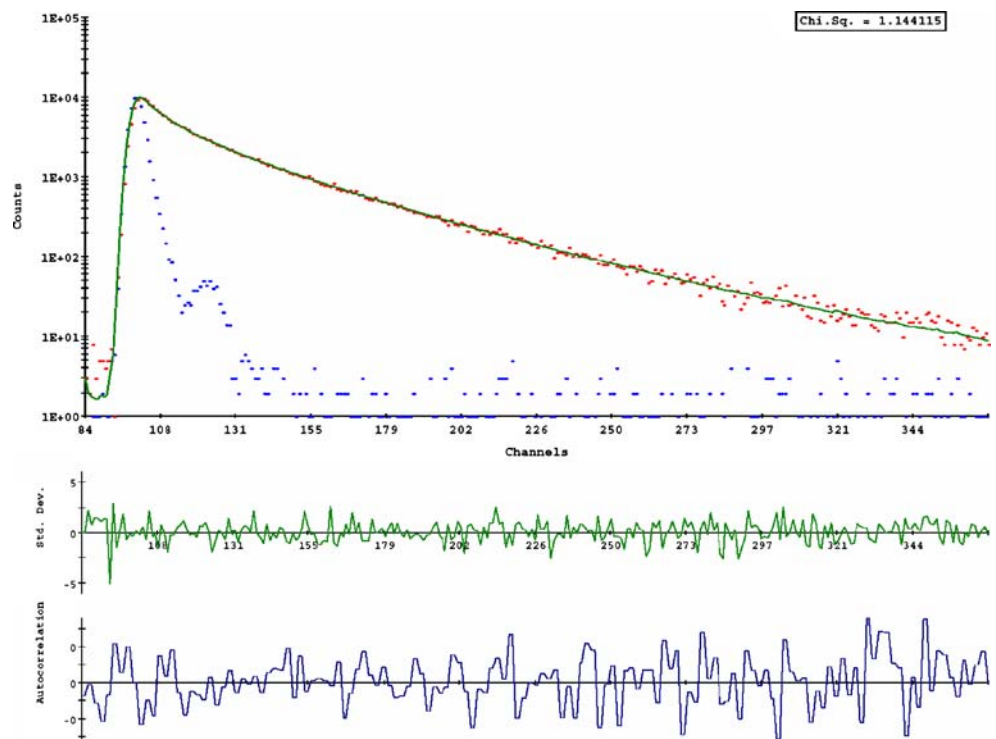
$$I(\lambda, t) = 0.35 e^{-t/0.413} + 0.56 e^{-t/2.096} + 0.09 e^{-t/5.45}$$

where 0.35, 0.56 and 0.09 are the pre-exponential factors and 0.413±0.022, 2.096±0.117 and 5.45±0.070 ns are the decay times and λ is the emission wavelength (330 nm) ($\chi^2=1.086$). $\lambda_{\text{ex}}=295$ nm. The weighted average fluorescence lifetime $\langle\tau\rangle=2.87$ ns was used to calculate the rotational correlation time from the Perrin plot.

The fluorescence intensity decay of TNS in presence of mutant CyPB_{W128A} can also be adequately represented by a sum of four exponentials (Fig. 5)

$$I(\lambda, t) = 0.1312 e^{-t/0.16} + 0.2127 e^{-t/1.72} + 0.4162 e^{-t/5.984} + 0.24 e^{-t/11.25}$$

Fig. 5 Fluorescence intensity decay of TNS-mutant cyclophilin B. $\lambda_{ex}=295$ nm and $\lambda_{em}=420$ nm



where 0.1312, 0.2127, 0.4162 and 0.24 are the pre-exponential factors and 0.16, 1.72, 5.984 and 11.25 ns the decay times ($\chi^2=1.145$). The lifetime equal to 0.16 ns corresponds to free TNS in solution and the longest lifetimes correspond to bound TNS. The weighted average fluorescence lifetime $\langle\tau\rangle=8.232$ ns was used to calculate the rotational correlation time from the Perrin plot. $\lambda_{ex}=295$ nm and $\lambda_{em}=420$ nm.

Dynamics of wild type cyclophilin B

Red-edge excitation spectra

Red-edge excitation spectra are used to monitor motions around the fluorophores [31]. If the dipole of the fluorophore microenvironment is able to relax before fluorophore emission, then this environment is considered to be fluid. This motion may induce that of the fluorophore. The emission maximum from a relaxed state does not change with the excitation wavelength, while an emission maximum from a non-relaxed state will depend on it. Emission maxima are usually compared when the spectra are symmetric. Otherwise, the centers of gravity should be compared.

The maximum of the fluorescence spectra of Trp residues of cyclophilin B is a function of the excitation wavelengths. At 295 nm, the emission maximum is located at 328 nm. It shifts to higher wavelengths (330 and 334 nm) when the excitation wavelengths are 300 and 305 nm, respectively (Fig. 6). This is taken as direct evidence that

the microenvironments of the Trp residues of wild type cyclophilin B show restricted motions. As the emission spectra are symmetric, we converted them to a wavenumber scale

$$\nu = 1/\lambda \tag{4}$$

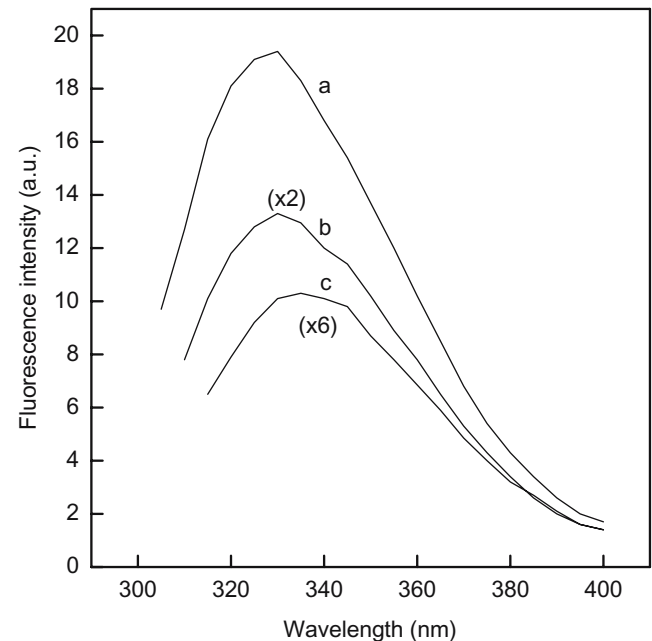


Fig. 6 Red-edge excitation spectra of wild type cyclophilin B. (a): $\lambda_{ex}=295$ nm; center of gravity=338 nm. (b): $\lambda_{ex}=300$ nm; center of gravity=342 nm. (c): $\lambda_{ex}=305$ nm; center of gravity=346 nm

then we compared the positions of their centers of gravity or mean wavenumber ν :

$$\nu = \frac{\sum I_i \nu_i}{\sum I_i} \quad (5)$$

where I_i is the fluorescence intensity at the wavenumber ν_i . The values of the center of gravity are $2.958 \times 10^4 \text{ cm}^{-1}$ (338 nm), $2.924 \times 10^4 \text{ cm}^{-1}$ (342 nm) and $2.890 \times 10^4 \text{ cm}^{-1}$ (346 nm) at λ_{ex} 295, 300 and 305 nm, respectively. The results obtained clearly indicate that the microenvironments of the Trp residues have restricted motions. Since we have two Trp residues, the results obtained are mean ones. Also, the results could be dominated by the Trp residue that contributes the most to the fluorescence emission, i.e., Trp-104 residue. Since the fluorophore microenvironment exhibits restricted mobility in wt cyclophilin B, i.e., the fluorophore would follow the motion of the protein, suggesting a rotational correlation time equal to that of the protein.

Steady-state anisotropy as a function of temperature

The rotational correlation time Φ_p of a hydrated sphere is obtained from the equation

$$\Phi_p(T) = 3.8 \eta(T) \times 10^{-4} M \quad (6)$$

where M ($= 21 \text{ kDa}$) is the protein molecular weight and η the viscosity of the medium.

Equation 6 yields a rotational correlation time of 8 ns at 20°C if the protein is spheric.

Steady state fluorescence anisotropy of Trp residues in wild type cyclophilin B ($\lambda_{\text{em}}=330 \text{ nm}$ and $\lambda_{\text{ex}}=300 \text{ nm}$) was performed at different temperatures. A Perrin plot representation (Fig. 7) based on Eq. 7 [32]

$$1/A = 1/A_o + \langle \tau \rangle / \Phi_R A_o = 1/A_o + (1/A_o) (1 + RT \langle \tau \rangle / \eta V) \quad (7)$$

where A and A_o are the anisotropies in the presence and the absence of rotational diffusion respectively, $\langle \tau \rangle = 2.23 \text{ ns}$, η , V and Φ_R are the mean fluorescence lifetime, the viscosity, the fluorophore rotational volume and its rotational correlation time, respectively. This plot enables us to obtain information concerning the motion of the fluorophore. When the fluorophore is tightly bound to the protein, its motion will correspond to that of the protein. In this case, Φ_R will be equal to Φ_p and A_o obtained experimentally with Eq. 7 will be equal to the limiting anisotropy measured at low temperature (-45°C). When the fluorophore exhibits significant motions when bound to the protein, Φ_R will represent an apparent rotational correlation time Φ_A . Φ_A will be the result of two motions, that of the protein and that of

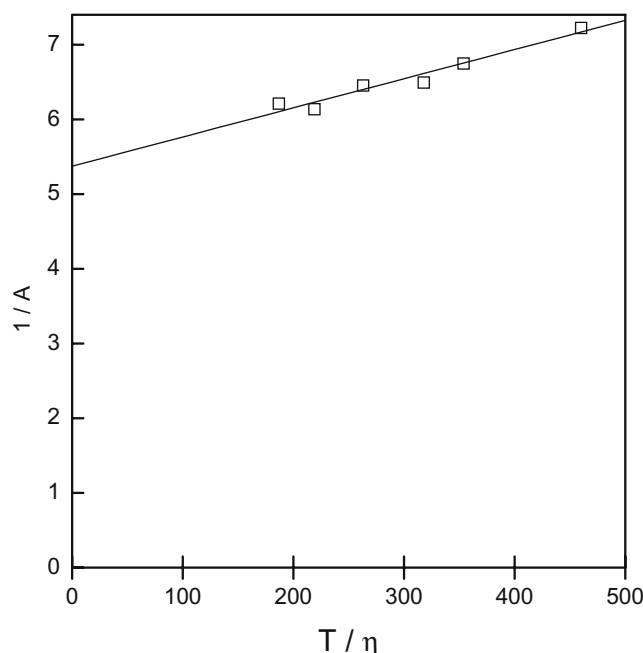


Fig. 7 Perrin plot of Trp residues of wild type cyclophilin B obtained at 20°C with $\lambda_{\text{ex}}=300 \text{ nm}$ and $\lambda_{\text{em}}=330 \text{ nm}$. The rotational correlation time obtained is equal to 10.95 ns and the extrapolated anisotropy A_o is found equal to 0.201

the segmental motion of the fluorophore. Also, in the presence of a segmental motion, the extrapolated value of A , $A(o)$ will be lower than the limiting anisotropy A_o .

The data for the Trp residues of wild type cyclophilin B are plotted in Fig. 7. The value of the extrapolated anisotropy ($A_o=0.201$) is close to the anisotropy (0.198) measured for Trp residues at low temperatures (-45°C) [33]. Also, the rotational correlation time Φ_R (10.5 ns at 20°C) obtained from the Perrin plot, is in the same range as that expected (8 ns) for cyclophilin B and thus indicates that the Trp residues follow the global motion of the protein.

Anisotropy results are in good agreement with those obtained by red-edge excitation spectra experiments, Trp residues are rigid in the protein. However, since we have two Trp residues, the results are mean ones and do not necessarily reflect the dynamics of each Trp residue.

Dynamics of Trp-104 residue of mutant cyclophilin B

Figure 8 shows the fluorescence emission spectra of Trp-104 residue of mutant cyclophilin B obtained at three excitation wavelengths. The emission maximum located at 329 nm at λ_{ex} 295 nm, shifts to 331 and 333 nm at λ_{ex} of 300 and 305 nm, respectively. Also, the centers of gravity of the spectra are 334, 337 and 342 nm, respectively. This result indicates that the microenvironment of Trp-104 residue shows restricted motions.

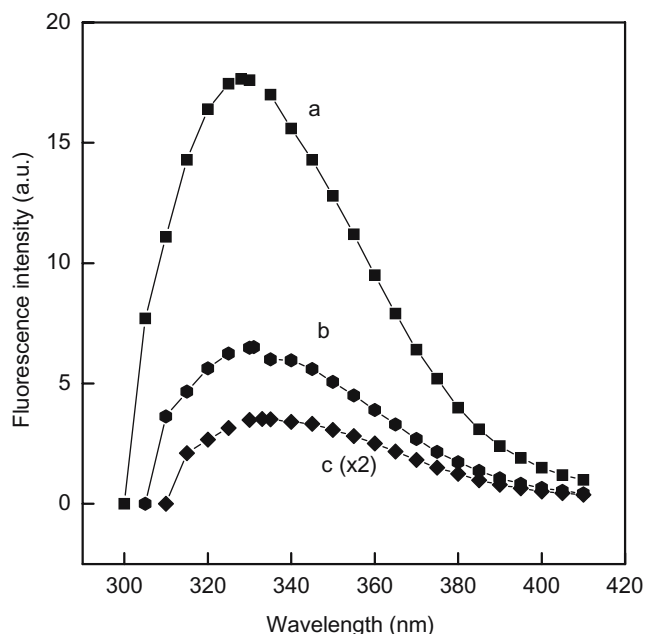


Fig. 8 Fluorescence spectra of Trp 104 of mutant cyclophilin B at λ_{ex} 295 (a), 300 (b) and 305 nm. λ_{max} are 329, 331 and 333 nm, respectively. The gravity centers of the spectra are 334, 337 and 342 nm, respectively. The bandwidth is 47 nm

The Perrin plot representation ($\lambda_{em}=330$ nm and $\lambda_{ex}=300$ nm) yields values of 0.204 and 8 ns (at 20°C) for the extrapolated anisotropy and the rotational correlation time, respectively (Fig. 9). These values indicate that the Trp-104 residue shows restricted local motions within the protein. This result is in good agreement with that observed with the red-edge excitation spectra, i.e., Trp-104 residue is rigid within its environment.

Binding parameters of TNS-cyclophilin B complex

In phosphate buffer, free TNS exhibits weak fluorescence. In the presence of cyclophilin B, an enhancement in the TNS fluorescence intensity appears with a maximum at 425 nm (λ_{ex} , 320 nm). This increase is the result of binding of the fluorophore to the protein. Also, the interaction between TNS and cyclophilin B induces a decrease in the fluorescence intensity of the Trp residue of the protein (λ_{ex} , 280 nm) (data not shown). In order to determine the binding parameters (stoichiometry and the association constant) of the TNS-cyclophilin B complex, a titration of a constant amount of the protein with the TNS was performed, following the intensity decrease of the Trp residue (Fig. 10). The concentration of TNS at saturation was determined at the intersection of the two asymptotes to the curve. Our plot indicates that 1 mol of TNS is bound to one mol of cyclophilin B.

The dissociation constant of the TNS-cyclophilin B complex was determined by fitting the data to Eq. 8

$$Flu = Flu_{(o)} - \Delta Flu \times \frac{[TNS]}{K_d + [TNS]} \tag{8}$$

with

$$[TNS]_{bound} = 1/2 \left\{ ([TNS] + [P_o] + K_d) - \left(([TNS] + [P_o] + K_d)^2 - 4[TNS][P_o] \right)^{0.5} \right\} \tag{9}$$

Where P_o is the protein concentration, Flu is the relative fluorescence intensity for a certain concentration of TNS, $Flu_{(o)}$ is the fluorescence intensity in absence of TNS, ΔFlu is the intensity decrease upon saturation with TNS and K_d the dissociation constant. K_d was found equal to $2.08 \pm 1.4 \mu M$, and $\Delta Flu = 0.41 \pm 0.06$.

Intensity quenching of Trp residue of $CyPB_{w128A}$ with TNS allowed us to determine the distance between Trp-104 residue and TNS. From the overlap of the emission spectrum of Trp-104 residue in $CyPB_{w124A}$ and absorption spectrum of TNS bound to cyclophilin (not shown), we have calculated the overlap integral J

$$J(\lambda) = \frac{\int_0^\infty F_D(\lambda) \cdot \epsilon_A(\lambda) \cdot \lambda^4 d\lambda}{\int_0^\infty F_D(\lambda) d\lambda} \tag{10}$$

J was found equal to $0.95 \times 10^{-4} M^{-1} cm^3$.

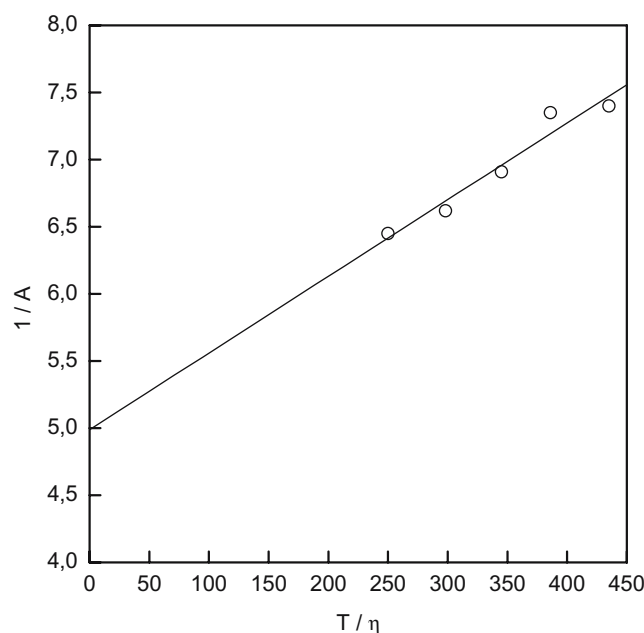


Fig. 9 Perrin plot of Trp 104 of the mutant cyclophilin B. λ_{ex} , = 300 nm and λ_{em} =330 nm. $A_o=0.2$ and $\tau_c=8$ ns at 20°C

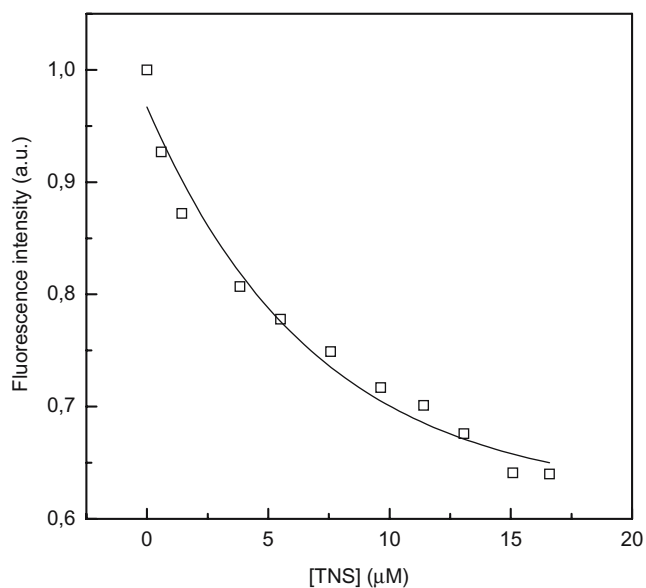


Fig. 10 Titration of 5.93 μM of mutant cyclophilin B with TNS. $\lambda_{\text{ex}}=295\text{ nm}$

The Forster distance R_0 (in cm) at which the efficiency of energy transfer E is 50% was calculated with Eq. 11:

$$R_0 = 9.78 \times 10^3 [\kappa^2 n^{-4} Q_d J(\lambda)]^{1/6} \quad (11)$$

where κ^2 is the orientation factor ($= 2/3$), n the refractive index ($=1.33$) and Q_d the average quantum yield ($= 0.049$). R_0 is calculated to be 20.36 \AA .

The value of the energy transfer efficiency E calculated at infinite concentrations of TNS was obtained by plotting $1/E$ as a function of $1/[\text{TNS}]$ (data not shown). E was found equal to 0.498.

The distance that separates the donor from the acceptor was calculated using Eq. 12:

$$R = R_0 \left(\frac{1 - E}{E} \right)^{1/6} \quad (12)$$

R was found equal to 17.8 \AA .

This value is lower than the diameter (33.5 \AA) of the pocket of the cyclophilin (Fig. 11) indicating that TNS is bound to a hydrophobic site within the protein pocket.

Dynamics of the TNS–cyclophilin B mutant complex

Red-edge excitation spectra

The maximum of the fluorescence spectra of TNS bound to CyPB_{w128A} is a function of the excitation wavelength. At 360 nm, the emission maximum is located at 426 nm. It shifts to higher wavelengths (434 and 444 nm) when the excitation wavelengths are 380 and 400 nm, respectively (data not shown). Also, the center of gravity of the spectrum shifts from 434 nm at $\lambda_{\text{ex}}=360\text{ nm}$ to 439 and

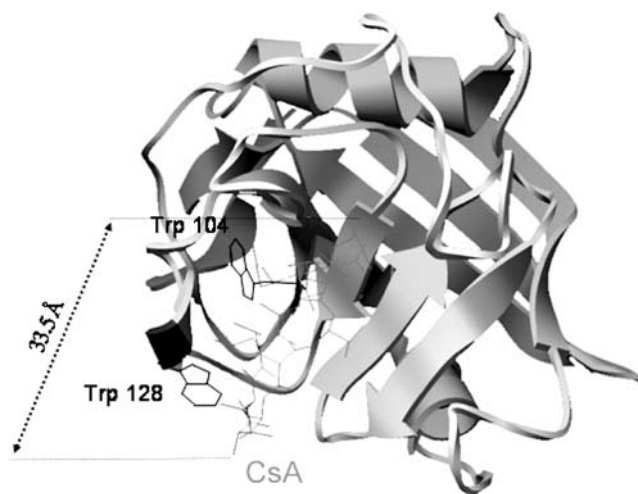


Fig. 11 Spatial structure of cyclophilin B

447 nm when the excitation wavelengths are 380 and 400 nm, respectively. These results are taken as direct evidence that TNS microenvironment exhibits restricted mobility in the cyclophilin. Therefore, the fluorophore could follow the motion of the protein suggesting a rotational correlation time equal to that of the protein.

Steady state anisotropy as a function of the temperature

Fluorescence anisotropy of the TNS–CyPB_{w128A} complex ($\lambda_{\text{ex}}=320\text{ nm}$ and $\lambda_{\text{em}}=425\text{ nm}$) was measured as a function of temperature. Data are plotted in Fig. 12. The value of the extrapolated anisotropy found from the Perrin plot is 0.322. This value is equal to that (0.321) measured

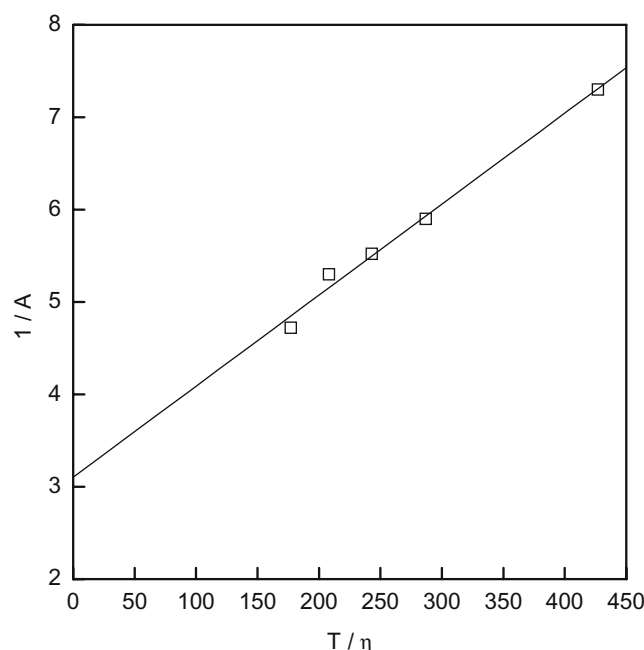


Fig. 12 Perrin plot of the complex TNS–mutant cyclophilin B. $\lambda_{\text{ex}}=320\text{ nm}$ and $\lambda_{\text{em}}=425\text{ nm}$. $A_0=0.322$ and $\tau_c=9.5\text{ ns}$ at 20°C

Table 1 Value of the emission to excitation ratio of wild type cyclophilin B and CyPB_{w128A} determined in comparison with free tryptophan in solution

Protein	R_{ex}^{em} at 280 nm	R_{ex}^{em} at 295 nm
Cyclophilin WT	0.341	0.2
CyPB _{w128A}	0.306	0.17

The value of the emission to excitation ratio for L-Trp in solution is taken as equal to 1

for TNS in propylene glycol at -65°C [34] and close to those measured for TNS when bound tightly to *Lens culinaris* agglutinin [18] and to α_1 -acid glycoprotein [35], (0.317 and 0.335, respectively). Thus, TNS has a restricted mobility on the cyclophilin. This result is in good agreement with that found in the red-edge excitation shift experiment.

The rotational correlation time ϕ_p (9.5 ns at 20°C), in the same range of that (9 ns) expected for cyclophilin B, indicates that TNS follows the global rotation of the protein.

Discussion

Comparison of the fluorescence spectra of Trp residues in wild type cyclophilin B and CyPB_{w128A} indicates that both 128 and 104-Trp residues participate to the emission of the protein, although this fluorescence seems to be dominated by that of Trp-104 residue. In fact, quantum yields of the two residues determined by two different methods show clearly that the quantum yield of Trp-104 residue (0.061) is 5 times that of Trp-128 residue (0.012). The low quantum yield of Trp-128 can be explained by the possibility of an electron transfer from the Trp residue to both Phe-67 and Asp-79 both present within a distance of 8.5 Å. The electron transfer toward the two neighboring amino acids decreases enormously the quantum yield of Trp-128 residue. The fact that the quantum yield of Trp-104 residue is very close in the wild type (0.054) and in the mutant (0.049) indicates the absence of energy transfer between Trp-128 and 104 residues in the wild type. This may be explained by the fact that the phenol rings of the two Trp residues are perpendicular one to each other (Fig. 11). Therefore, electron transfer from Trp-128 to Phe-67 and Asp-79 could be a cause of the low value of the quantum yield of Trp-128 residue. However, another interpretation of the weak fluorescence of Trp-128 may also exist. Fluorescence quantum yield compares the emitted photons to the absorbed ones. However, there is no indication up to now that all the absorbed photons participate in the excitation process. In fact, we recently find out that absorption of

aromatic amino acids whether free in solution or present within a protein are not equivalent to excitation [36]. In general, one is used to consider the absence of fluorescence from a fluorophore as the result of excited state energy dissipation into the medium via different processes that compete with fluorescence. However, can't we consider the case where fluorophore does not emit simply because it was not excited? The lack of excitation would be the result of structural rearrangement within the fluorophore microenvironment. Therefore, we introduced a new parameter we called the emission to excitation ratio R_{ex}^{em} and which is equal to the energy of the emitted light over the energy used to excite the fluorophore:

$$R_{ex}^{em} = \frac{\text{number of emitted photons}}{\text{number of photons used to excite the fluorophore}} \quad (13)$$

Thus, R_{ex}^{em} is calculated by comparing the emission spectrum to the excitation intensity at the excitation wavelength instead of the optical density as it is the case when the quantum yield is determined. The value of R_{ex}^{em} is obtained by taking free L-Trp as reference with a value of R_{ex}^{em} equal to 1. Determination of R_{ex}^{em} is much more accurate than the quantum yield Φ since the value of R_{ex}^{em} is independent of the optical density of the studied sample.

The emission to excitation ratio R_{ex}^{em} , to the difference of Φ , yields direct information on whether a fluorophore is excited or not. In fact, in proteins, when the value of R_{ex}^{em} at 295 is lower than at 280 nm, this means that excitation of tyrosine occurs at 280 nm although tyrosine contribution to the protein fluorescence could be very low or absent because of many processes such as for example energy transfer to neighboring amino acids or to tryptophan residues.

Table 1 displays the values of R_{ex}^{em} obtained for cyclophilin B wild type and CyPB_{w128A} at λ_{ex} equal to 280 and 295 nm. The values of R_{ex}^{em} at 280 nm for both proteins are much higher than those obtained at 295 nm. This means that excitation of the tyrosine residues of the cyclophilin is occurring. The most interesting are the ratios calculated at each wavelength between the two proteins (Table 2).

$\frac{R_{ex}^{em} \text{ at 280 nm of the mutant}}{R_{ex}^{em} \text{ at 280 nm of the wild type}}$ is equal to 0.88 while the same ratio determined at 295 nm is found equal to 0.85. Thus, since the ratios are equal at both wavelengths, this means that energy transfer between the two Trp residues is not occurring, a conclusion in good agreement with the fact that the phenol rings of the two Trp residues are perpendicular one to each other (Fig. 11), and thus emission of cyclo-

Table 2 Ratios of the emission to excitation ratio R_{ex}^{em} of wild type cyclophilin B and mutant cyclophilin B calculated at 280 and 295 nm

$\frac{R_{ex}^{em} \text{ at 280 nm of CyPBw128A}}{R_{ex}^{em} \text{ at 280 nm of cyclophilin wild type}}$	$\frac{R_{ex}^{em} \text{ at 295 nm of CyPBw128A}}{R_{ex}^{em} \text{ at 295 nm of cyclophilin wild type}}$
0.88	0.85

philin B is dominated by Trp-104 residue. Therefore, excitation of Trp-128 residue is weak, a conclusion that is proved by the values of $R_{\text{ex}}^{\text{em}}$ at 295 nm of the two proteins (0.17 and 0.2 for the mutant and the wild type, respectively). In this case, the weak excitation of Trp-128 residue generates a low quantum yield. In the absence of energy transfer between Trp-104 and Trp-128 residues, one can calculate the value of $R_{\text{ex}}^{\text{em}}$ of Trp-128 residue at 295 nm by subtracting the value of the mutant (0.17) from that of the wild type (0.2). $R_{\text{ex}}^{\text{em}}$ of Trp-128 residue is thus equal to 0.03 at 295 nm and is 15% that of the wild type. This ratio is very close of that (19%) found for the quantum yields indicating clearly that the low quantum yield of Trp-128 is simply the result of its low light excitation.

We also investigated the dynamics properties of the Trp residues in the wild and mutant cyclophilins B by fluorescence anisotropy studies and red edge excitation spectra method. The two techniques are complementary since the red-edge excitation spectra method allows to study the flexibility of the microenvironment while anisotropy studies allow to monitor the dynamics of the fluorophore itself. The results obtained show that the microenvironments of the Trp residues are not flexible and the Trp residues display restricted motions. The two Trp residues are present in the hydrophobic pocket of the protein and our data seems to indicate that this site does not have any residual motion.

Although, red-edge experiments and anisotropy data show the absence of any significant local motions of Trp residues, a switch of the molecule around its axis by a certain angle cannot be ruled out. This motion and its importance would depend mainly on the structure of the molecule itself.

Results obtained on the wild type and on the mutant are identical. This may be explained by the fact that in both proteins we are mainly observing the fluorescence of the Trp-104 residue. Trp-128 residue does not participate significantly to the fluorescence of cyclophilin B.

The value of 0.48 found for the energy transfer efficiency E suggests that energy transfer mechanism from Trp residue to TNS occurs within a time close to the fluorescence lifetime. The constant rate of the energy transfer (k_t) can be calculated from Eqs. 14 and/or 15:

$$k_t = (1/\langle \tau \rangle) (R_o/R)^6 \quad (14)$$

and

$$k_t = 1/\langle \tau \rangle - 1/\tau_r \quad (15)$$

where τ_r is the radiative lifetime.

The radiative rate constant k_r

$$k_r = 1/\tau_r = Q/\langle \tau \rangle \quad (16)$$

is equal to $0.02019 \times 10^9 \text{ s}^{-1}$.

Equations 15 and 16 yield very close values for k_t , $0.395 \times 10^9 \text{ s}^{-1}$ and $0.376 \times 10^9 \text{ s}^{-1}$, respectively. We notice that k_t is $48.4 \pm 0.3\%$ of the sum of the rate constants of Eq. 2 confirming the value of 49.8% obtained for E .

50% energy transfer between Trp and TNS cannot be considered as a highly efficient one. Many factors contribute to this fact such as the position of TNS inside cyclophilin B pocket and thus the relative Tryptophan dipole–TNS dipole orientation. From the data we obtained, this relative orientation is not appropriate for a highly efficient energy transfer. Since we do not know the real relative orientation of the emission dipole of the Trp residue and of the absorption dipole of TNS, the value of κ^2 could be different from 2/3. For 100% energy transfer between the two fluorophores, the value of κ^2 is equal to 4. In this case, R is equal to 30 Å, a value lower than the diameter of the pocket. However, since energy transfer is around 50% efficient, the real value of κ^2 is much lower than 4. If κ^2 is taken as equal to 2, the value of R is found equal to 27 Å. Thus, the value found by taking κ^2 equal to 2/3 is a good approximation although errors on the determination of this value do exist.

CsA binding site of cyclophilin B is formed by a pocket where the two Trp residues are present and where TNS can bind inducing by that an important energy transfer from Trp-104 residue to the extrinsic fluorophore. Red-edge excitation spectra and anisotropy steady have shown that TNS binding site is rigid and the microenvironment of the fluorophore does not display important flexibility. This result is in good agreement with that obtained with the Trp residues, i.e. hydrophobic pocket of cyclophilin B does not display significant motions.

References

- Galat A (1993) Peptidylproline *cis*–*trans*-isomerases: immunophilins. Eur J Biochem 216:689–707
- Fischer G, Wittmann-Liebold B, Lang K, Kiefhaber T, Schmid FX (1989) Cyclophilin and peptidyl-prolyl *cis*–*trans* isomerase are probably identical proteins. Nature 337:476–478
- Price ER, Zydowsky LD, Jin M, Baker CH, McKeon, FD, Walsh CT (1991) Human cyclophilin B: A second cyclophilin gene encodes a peptidyl-prolyl isomerase with a signal sequence. Proc Natl Acad Sci 88:1903–1907
- Friedman J, Weissman I (1991) Two cytoplasmic candidates for immunophilin action are revealed by affinity for a new cyclophilin: one in the presence and one in the absence of CsA. Cell 66:799–806
- Hasel KW, Glass JR, Godbout M, Sutcliffe JG (1991) An endoplasmic reticulum-specific cyclophilin. Mol Cell Biol 11:3484–3491
- Spik G, Haendler B, Delmas O, Mariller C, Chamoux M, Maes P, Tartar A, Montreuil J, Stedman K, Kocher HP (1991) A novel secreted cyclophilin-like protein (SCYLP). J Biol Chem 266:10735–10738
- Connern CP, Halestrap AP (1992) Purification and N-terminal sequencing of peptidyl-prolyl *cis*–*trans*-isomerase from rat liver

- mitochondrial matrix reveals the existence of a distinct mitochondrial cyclophilin. *Biochem J* 284:381–385
8. Kay JE (1992) Mitochondrial cyclophilins. *Biochem J* 288:1074–1075
 9. Montague JW, Hughes FM Jr., Cidlowski, JA (1997) Native recombinant cyclophilins A, B, and C degrade DNA independently of peptidylprolyl *cis*–*trans* isomerase activity: potential roles of cyclophilins in apoptosis. *J Biol Chem* 272:6677–6684
 10. Woodfield K, Ruck A, Brdiczka D, Halestrap AP (1998) Direct demonstration of a specific interaction between cyclophilin-D and the adenine nucleotide translocase confirms their role in the mitochondrial permeability transition. *Biochem J* 336:287–290
 11. Fisher G, Bang H (1985) The refolding of urea-denatured ribonuclease A is catalyzed by peptidyl–prolyl *cis*–*trans* isomerase. *Biochim Biophys Acta* 828:39–42
 12. Schmid FX, Mayr LM, Mücke M, Schönbrunner, ER (1993) Prolyl isomerases: role in protein folding. *Adv Protein Chem* 44:25–66
 13. Handschumacher RE, Harding MW, Rice J, Drugge RJ (1984) Cyclophilin: a specific cytosolic binding protein for cyclosporin A. *Science* 226:544–547
 14. Carpentier M, Allain F, Haendler B, Denys A, Mariller C, Benaissa M, Spik G (1999) Two distinct regions of cyclophilin B are involved in the recognition of a functional receptor and of glycosaminoglycans on T lymphocytes. *J Biol Chem* 274:10990–10998
 15. Mikol V, Kallen J, Walkinshaw MD (1994) X-ray structure of a cyclophilin B/cyclosporin complex: comparison with cyclophilin A and delineation of its calcineurin-binding domain. *Proc Natl Acad Sci USA* 91:5183–5186
 16. Golbik R, Eble J, Ries A, Kuhn K (2000) The spatial orientation of the essential amino acid residues arginine and aspartate within the $\alpha_1 \beta_1$ integrin recognition site of collagen IV has been resolved using fluorescence resonance energy transfer. *J Mol Biol* 297:501–509
 17. Dong WJ, Robinson JM, Xing J, Umeda PK, Cheung HC (2000) An interdomain distance in cardiac troponin C determined by fluorescence spectroscopy. *Protein Sci* 9:280–289
 18. Albani JR (1996) Dynamics of *Lens culinaris* agglutinin studied by red-edge excitation spectra and anisotropy measurements of 2-*p*-toluidinylnaphthalene-6-sulfonate (TNS) and of tryptophan residues. *J Fluoresc* 6:199–208
 19. Mikes V, Milat M-L, Ponchet M, Panabières F, Ricci P, Blein J-P (1998) Elicitins, proteinaceous elicitors of plant defense, are a new class of sterol carrier proteins. *Biochem Biophys Res Commun* 245:133–139
 20. Chen RF (1967) Fluorescence quantum yields of tryptophan and tyrosine. *Anal Lett* 1:35–42
 21. Lakowicz JR, Cherek H (1981) Phase-sensitive fluorescence spectroscopy. A new method to resolve fluorescence lifetimes or emission spectra of components in a mixture of fluorophores. *J Biochem Biophys Methods* 5:19–35
 22. D'Auria S, Gryczynski Z, Gryczynski I, Rossi M, Lakowicz JR (2000) A protein biosensor for lactate. *Analytical Biochemistry* 283:83–88
 23. Sanger F, Nicklen F, Coulson, AR (1977) DNA sequencing with chain-terminating inhibitors. *Proc Natl Acad Sci USA* 74:5463–5467
 24. Allain F, Spik G (1995) In: Haerberli A (ed) *Human protein data*. VCH Verlagsges, mbH, Weinheim
 25. McClure WO, Edelman GM (1966) Fluorescent probes for conformational states of proteins. I. Mechanism of fluorescence of 2-*p*-toluidinylnaphthalene-6-sulfonate, a hydrophobic probe. *Biochemistry* 5:1908–1918
 26. Lakowicz JR (1999) *Principles of fluorescence spectroscopy*. Plenum, New York
 27. Albani JR (2007) *Principles and applications of fluorescence spectroscopy*. Blackwell, Oxford
 28. Parker CA, Rees WT (1960) Correction of fluorescence spectra and measurement of fluorescence quantum efficiency. *Analyst* 85:587–600
 29. Burstein EA, Vedenkina NS, Ivkova MN (1973) Fluorescence and the location of tryptophan residues in protein molecules. *Photochem Photobiol* 18:263–279
 30. Albani JR (1997) Binding effect of progesterone on the dynamics of α_1 -acid glycoprotein. *Biochim Biophys Acta* 1336:349–359
 31. Demchenko AP (1982) On the nanosecond mobility in proteins. Edge excitation fluorescence red shift of protein-bound 2-*p*-toluidinylnaphthalene)-6-sulfonate. *Biophys Chem* 15:101–109
 32. Weber G (1952) Polarization of the fluorescence of macromolecules. 1. Theory and experimental method. *Biochem J* 51:145–155
 33. Albani JR (2004) *Structure and dynamics of macromolecules: absorption and fluorescence studies*. Elsevier, Amsterdam
 34. Lakowicz JR, Gratton E, Cherek H, Maliwal BP, Laczkó G (1984) Determination of time-resolved fluorescence emission spectra and anisotropies of a fluorophore–protein complex using frequency-domain phase-modulation fluorometry. *J Biol Chem* 259:10967–10972
 35. Albani J (1992) Motions studies of the human α_1 -acid glycoprotein (orosomuroid) followed by red-edge excitation spectra and polarization of 2-*p*-toluidinylnaphthalene-6-sulfonate (TNS) and of tryptophan residues. *Biophys Chem* 44:129–137
 36. Albani JR (2007) New insights in the interpretation of tryptophan fluorescence: origin of the fluorescence lifetime and characterization of a new fluorescence parameter in proteins: the emission to excitation ratio. *J Fluoresc* 17:406–417